Acoustics'08 Paris
June 29-July 4, 2008
www.acoustics08-paris.org

On determination of microphone response and other parameters by a hybrid experimental and numerical method

Salvador Barrera-Figueroa[a], Finn Jacobsen[b] and Knud Rasmussen[a]

[a]Danish Fundamental Metrology, Matematiktorvet 307, 2800 Kgs. Lyngby, Denmark
[b]Acoustic Technology Department, Technical University of Denmark, Ørsted Plads, B352, DK-2800 Lyngby, Denmark
sbf@dfm.dtu.dk

Typically, numerical calculations of the pressure, free-field and random-incidence response of a condenser microphone are carried out on the basis of an assumed displacement distribution of the diaphragm of the microphone; the conventional assumption is that the displacement follows a Bessel function. This assumption is probably valid at frequencies below the resonance frequency. However, at higher frequencies the movement of the membrane is heavily coupled with the damping of the air film between membrane and back plate, and with resonances in the back chamber of the microphone. A solution to this problem is to measure the velocity distribution of the membrane by means of a non-contact method, such as laser vibrometry. The measured velocity distributions can be used together with a numerical formulation such as the Boundary Element Method for estimating the microphone response and other parameters such as the acoustic centers. In this work, a hybrid method is presented. The velocity distributions of a number of condenser microphones were measured using a laser vibrometer. This measured velocity distribution was used for estimating the microphone responses and parameters. The agreement with experimental data is good. This method can be used as an alternative for validating the parameters of the microphones determined by classical calibration techniques.

1 Introduction

The numerical calculation of pressure, free-field, and random-incidence responses of microphones has become a popular method for validating results obtained experimentally. Furthermore, numerical calculations are used sometimes to complement experimental results at frequencies where the experimental methods might yield unreliable results [1-5].

However, the numerical calculations are carried out under a number of assumptions that are not always fully realistic. While complex geometries and configurations can easily be simulated, other parameters such as the velocity distribution of the membrane of a microphone are assumed to have a well defined analytical form. However, experimental results indicate that the velocity of the membrane may have another quite different shape.

There have been some attempts to solve the coupled model of a condenser microphone numerically [6-8]. However, to determine the velocity of the membrane has proven to be an elusive task. Behler and Vorländer proposed an alternative solution which consists of measuring the velocity of the membrane of the microphone using a non-contact method: a laser vibrometry, and to use these measurements in a numerical model of the microphone [9].

This paper presents an investigation on the possibility of using the measured velocity of the membrane of a microphone for the determination of quantities of the microphone by means of a hybrid numerical-experimental method. The velocity of the membrane of different types of microphones was measured using a laser vibrometer. This velocity was used in a Boundary Element Method (BEM) model of a microphone as a boundary condition at the membrane of the microphone. The acoustic centers, free-field corrections, pressure sensitivities, and directivity indexes of some types of microphones were calculated from using the estimated pressure on the membrane and on the sound field surrounding the microphone.

2 Theoretical background

A condenser microphone is a reciprocal transducer the behavior of which can be defined in terms of the equations of a four port electro-acoustic network. The open-circuit pressure sensitivity of the microphone, M_p, can be determined from:

$$M_\mathrm{p} = \frac{u_{i=0}}{p} = -\frac{q_{p=0}}{i}, \tag{1}$$

where $u_{i=0}$ is the open-circuit voltage, $q_{p=0}$ is the volume velocity under no acoustic load conditions, p is the pressure on the acoustic terminals, and i is the current. A graphic representation of the network of the microphone is shown in Fig. 1.

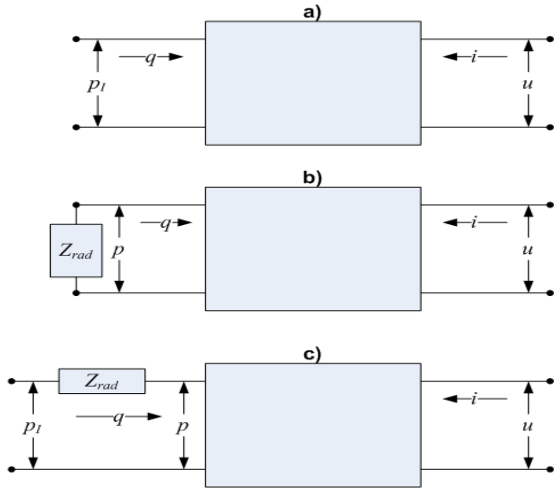

Figure 1. Network representation of a microphone: a) unloaded microphone; b) microphone as a sound source; and c) microphone as a receiver.

If the microphone is acting as a sound source, the ratio of the volume velocity to the current will be affected by the load of the radiation impedance:

$$-\frac{q}{i} = M_\mathrm{p}\frac{Z_\mathrm{a}}{Z_\mathrm{a}+Z_\mathrm{rad}}, \tag{2}$$

where Z_a is the acoustic impedance of the microphone, and Z_rad is the radiation impedance.

2.1 Acoustic center

The concept of acoustic center has been widely used in the development and practical realization [10-13] of free-field reciprocity calibration of microphones. The acoustic center of a microphone is defined as follows: "For a sound emitting transducer, for a sinusoidal signal of given frequency and for a specified direction and distance, the point from which the approximately spherical wavefronts, as observed in a small region around the observation point, appear to diverge" [13].

The discussion may be simplified if the microphones are regarded as axi-symmetric sources observed from positions on the axis of symmetry. Under this assumption, the acoustic center must be somewhere on the axis. If the amplitude of the sound pressure is plotted as a function of the distance, a straight line can be fitted over the region of concern. Thus, the position of the acoustic center, $x(k, r)$, can be determined using the following expression

$$x(k,r) = r + |p(r)| \Big/ \left(\partial |p(r)| / \partial r\right), \quad (3)$$

where k is the wave number, r is the axial distance from the diaphragm of the microphone, $p(r)$ is the sound pressure as a function of distance, and the rate of change, $\partial |p(r)| / \partial r$, must be estimated by any available means, for example by using least squares fitting [3].

2.2 Free-field correction

The free-field correction, C_{ff}, is defined as the logarithmic ratio of the free-field sensitivity to the pressure sensitivity:

$$C_{\mathrm{ff}} = 10\log\left\{|M_{\mathrm{ff}}|^2 \Big/ |M_{\mathrm{p}}|^2\right\}, \quad (4)$$

where M_{ff} is the free field sensitivity, and M_{p} is the pressure sensitivity of a microphone. Alternatively, the free-field correction can be also calculated using [1]

$$C_{\mathrm{ff}} = 20\log_{10}\left\{\int \left(p(r)/p_0\right)\cdot v(r) r dr \Big/ \int v(r) r dr\right\}, \quad (5)$$

where $p(r)$ is the pressure on the membrane as a function of the radius r, $v(r)$ is the velocity of the membrane as a function of r, and p_0 is the undisturbed incident pressure. The calculation of the pressure is carried out using an iterative procedure that involves the estimate of the acoustic impedance of the microphone by means of any available method.

2.3 Directivity Index

The directivity factor, Q, at the frequency f is defined as [14]:

$$Q(f) = \frac{4\pi |H(f,\theta_0,\phi_0)|^2}{\int_0^{2\pi}\int_0^{\pi} |H(f,\theta,\phi)|^2 \sin\theta d\theta d\phi}, \quad (6)$$

where $H(f, \theta, \phi)$ is the frequency response at the frequency f and the angles θ and ϕ. The index 0 indicates the axial direction. Assuming that the microphone is rotationally symmetrical, and substituting the integral by discrete series, Eq. (6) simplifies to

$$Q(f) = \frac{2|H(f,\theta_0)|^2}{\sum_{n=1}^{\pi/\Delta\theta} |H(f,\theta)|^2 \sin\theta_n \Delta\theta}. \quad (7)$$

The directivity index, D, is the directivity factor expressed in logarithmic fashion, i.e.,

$$D = 10\log Q. \quad (8)$$

3 Experimental setup

The velocity of the membrane has been measured using a laser vibrometer Polytech XXXX. The microphone membrane was excited using a reciprocity apparatus, Brüel & Kjær type 5998. The voltage on the terminals of the reference impedance on the transmitter unit, Brüel & Kjær type ZE0796, and the output of the vibrometer was measured using a Brüel & Kjær PULSE analyzer. Figure 2 shows a block diagram of the measurement setup. Figure 3 shows a picture of the vibrometer and the microphone mounted on the positioning rig.

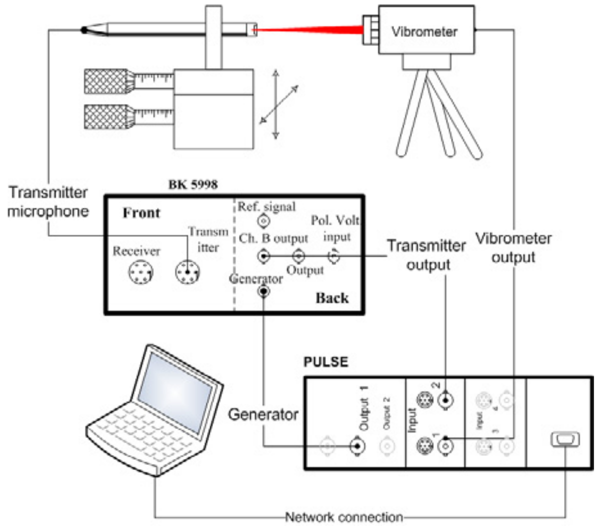

Figure 2. Block diagram of the measurement system.

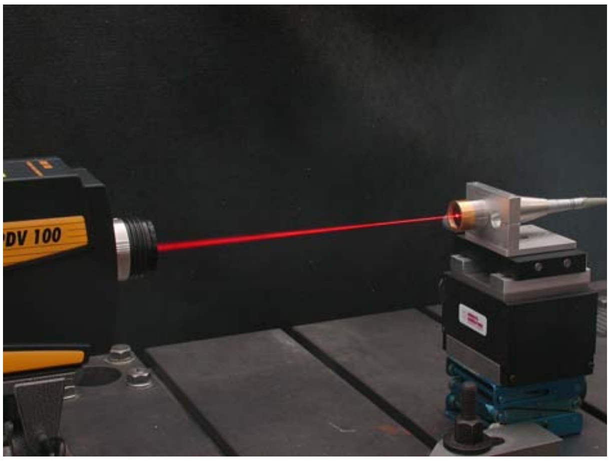

Figure 3. Picture of the measuring setup. The laser beam was measuring the velocity at a point on the membrane.

The signal used for exciting the microphone was pseudo-random noise with a bandwidth of 25.6 kHz, and 6400 lines. The laser vibrometer can measure up to 24 kHz. Several types of microphones were measured: 1-inch and ½-inch Laboratory and Working Standard microphones (LS1, WS1, LS2 and WS2, respectively). Additionally, a set of special condenser microphones was examined. The geometry of the special microphones are similar to a one-inch Working Standard microphone (WS1). However, these microphones do not have holes or slits on the back-plate. Therefore, the damping is larger than in a typical WS1 microphone.

4 BEM modeling

The geometry used in the BEM calculations is shown in Fig. 4. The semi-infinite rod was approximated using a cylindrical rod with a length of 60 cm with a hemispherical back-end. This will introduce a small disturbance in the simulated results because of the reflections from the back of the rod. However, because of the length of the rod, they are expected that to have a small amplitude. The frequency range used in the calculations is from 1 kHz to 20 kHz for LS1 microphones and from 2 kHz to 40 kHz for LS2 microphones. The size of the smallest element in the axisymmetric mesh is 2.5 mm and 1.5 mm for LS1 and LS2 microphones respectively. Thus, there will be at least 4 elements per wavelength at the highest frequency.

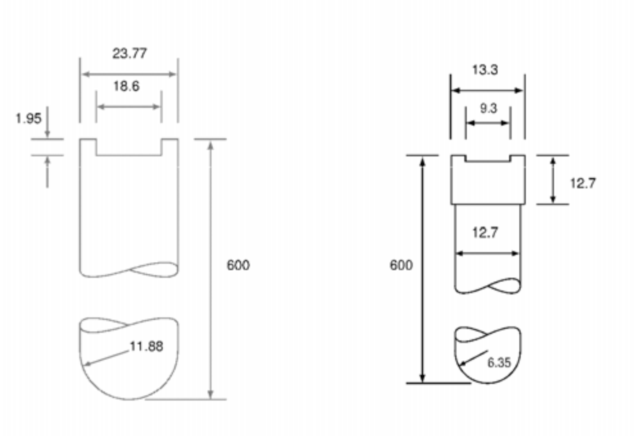

Figure 4. Geometry of LS1 and LS2 microphones used in the simulations.

In order to avoid the non-uniqueness problem a random CHIEF point has been added in the interior of the geometry as described in reference [15], and the calculation have been checked by determining the condition numbers of the BEM matrices [16] and by repeating calculations with small frequency shifts.

Depending on the quantity to be determined, the microphone acts as receiver or as a source. When the microphone acts only as a source, the radiation problem is solved by assigning the measured velocity to the membrane of the microphone. In the scattering problem, the structural coupling between the membrane and the scattered sound field is solved using a iterative procedure.

5 Results and discussion

5.1 Movement of the membrane

Figures 5 and 6 show the results of the velocity of the membrane of two different types of microphones at different frequencies.

It can be seen in Fig. 5 that the shape of the movement of the membrane of an LS1 microphone is similar to a parabola at frequencies below 5 kHz. Above that frequency and around the resonance frequency, the shape deviates from the assumed parabola. This departure becomes more obvious at higher frequencies. From 14 kHz and above, the center of the membrane flattens, and no longer looks as a parabola, nor as any other analytical shape. It is apparent that above 20 kHz, the center of the membrane does not move as much as a rim between the center and the fixed perimeter of the membrane. The velocity profiles are the result of the interaction between the membrane and the backplate of the microphone. The positions of the maxima coincide with the position of the holes and the recess on the backplate.

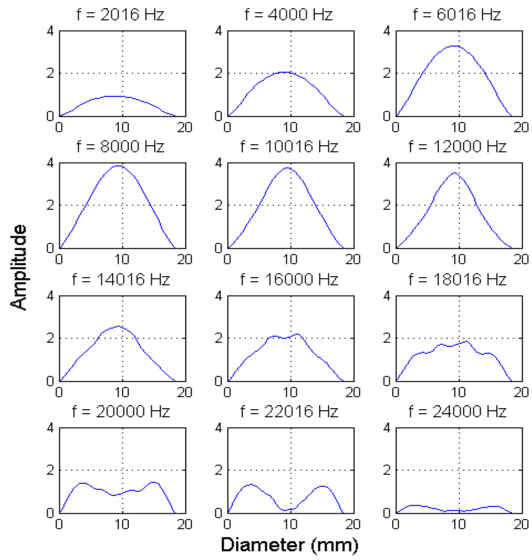

Figure 5. Velocity of the membrane of a LS1 microphone at several frequencies.

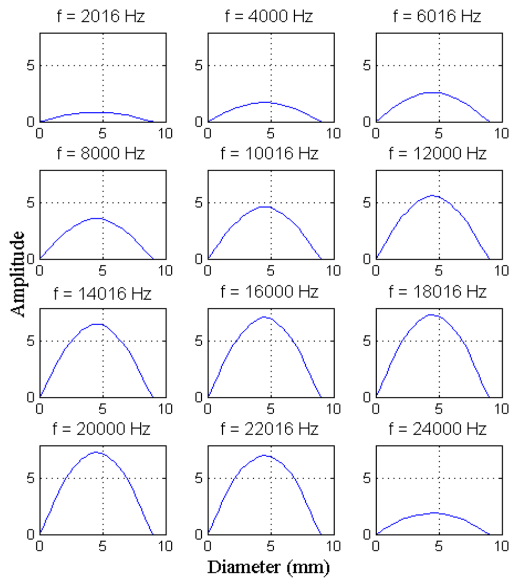

Figure 6. Velocity of the membrane of a LS2 microphone at several frequencies.

The movement of the membrane of an LS2 microphone shows a different behavior (Fig. 6). It can be seen the shape is more regular in the same frequency interval, even around the resonance frequency (approximately 18 kHz). Only above the resonance frequency, the shape seems to flatten slightly.

From the above results, it seems to be difficult to make any *a-priory* assumption of the movement of the membrane above the resonance frequency of the microphones.

5.2 Pressure sensitivity

Figure 7 shows the normalized pressure sensitivity of one of a LS1 microphone compared with the experimental response obtained using the reciprocity technique.

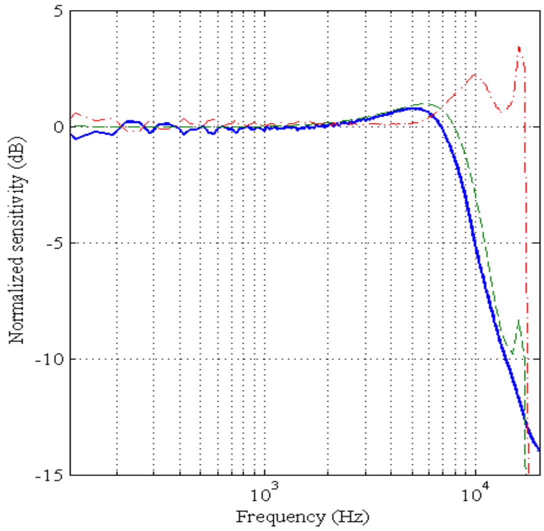

Figure 7. Normalized pressure response of a LS1 microphone. Dashed line: estimate obtained from reciprocity; solid line: estimate from the hybrid method; dash-dotted line: difference between estimates.

The difference between the responses is caused by the load of the radiation impedance on the acoustic impedance of the microphone (see Eq.(2)). This difference coincides with the difference observed in the literature [17].

5.3 Acoustic center

Figure 8 shows the acoustic center of an LS1 microphone determined from numerical BEM calculations using a parabolic, a Bessel like function and the measured velocity distribution. The results are compared to data obtained experimentally from reciprocity measurements.

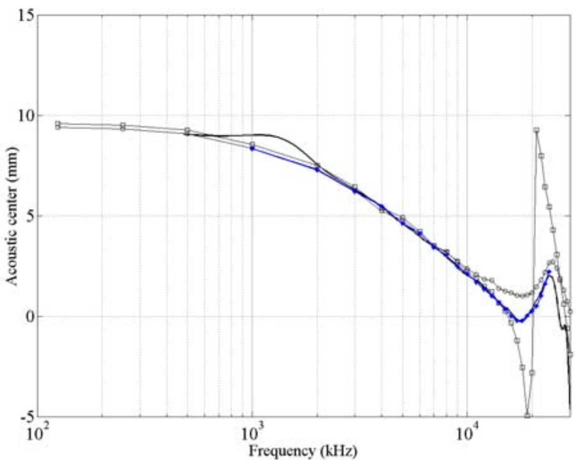

Figure 8. Acoustic center of a LS1 microphone. Solid line: experimental estimate; line with square markers: numerical estimate assuming a Bessel-like movement; line with circular markers: numerical estimate obtained assuming a uniform velocity; and line with star-markers: estimate from the hybrid method.

It can be seen in figure 8 that the agreement between measured data and the BEM calculations using the measured velocity distribution is extremely good in the whole frequency range. This result suggests that the sound field calculated using the hybrid method is more accurate than calculations based on any other assumption, especially at high frequencies.

5.4 Free-field correction

Figure 9 shows the free-field correction of LS1 and LS2 microphones determined experimentally, and using the hybrid method.

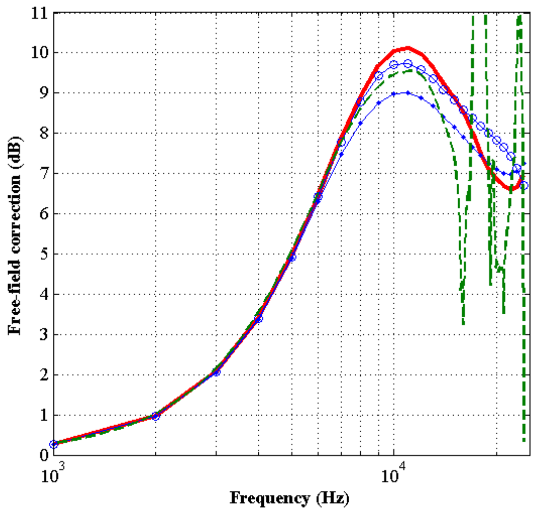

Figure 9. Free-field correction of LS1 microphones. Solid line: estimate from the hybrid method; dashed line: experimental estimate; line with circular markers: numerical estimate assuming parabolic movement; line with dot markers: numerical estimate assuming uniform movement.

The agreement between the experimental result, and the estimate obtained with the hybrid method is not very good around and above resonance frequency. The reason for this can be that in order to determine the correction, one has to use values of the acoustic impedance of the microphone. In this case, a lumped-parameter approximation was used. This approximation is limited to frequencies below the resonance frequency, therefore this approximation is degrading the results of the hybrid method.

5.5 Directivity Index

Figure 10 shows the directivity index of LS1 and LS2 microphones. It is also evident from the figure that the directivity index calculated with the measured velocity distribution follows the experimental estimate better. This is particularly clear for the case of the LS1 microphone, in which the experimental index shows a change of slope around 15 kHz. This behavior cannot be obtained using a parabolic movement in the simulations.

In the case of the LS2 microphones, the difference between the experimental and the hybrid method coincide very well up to 20 kHz. Nothing can be said at higher frequencies because these frequencies lie outside the measurement range of the laser vibrometer.

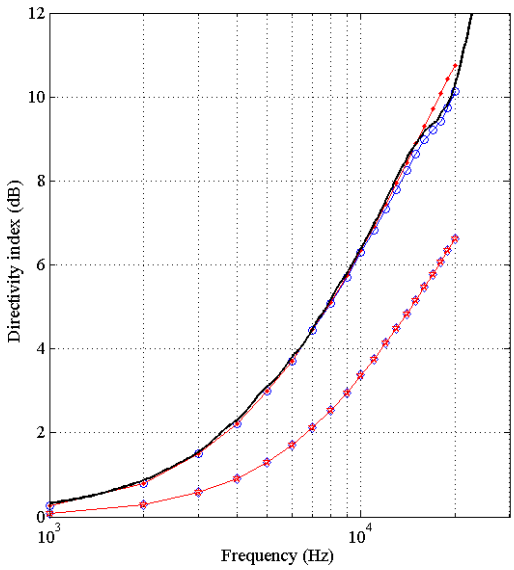

Figure 10. Directivity index of LS1 and LS2 microphones determined experimentally, and with the hybrid method. Solid line: Experimental LS1; line with circular markers: hybrid method; line with solid circular markers: numerical assuming uniform movement; line with star markers: hybrid method; line with diamond markers: numerical assuming uniform movement.

6 Conclusions

The velocity of the membrane of different types of microphones measured with a laser vibrometer indicates that no general assumption can be made for the behavior of all microphones. The preliminary results of the pressure sensitivity, the acoustic center, the free-field correction, and the directivity index obtained with the hybrid method are in good agreement with the experimental results obtained by traditional methods when the quantity in question is determined directly. Therefore, the hybrid method can be used for validating new experimental setups. Furthermore, the results of the hybrid method can be used in production environments to check the responses of a prototype microphone without the need of a complete calibration setup. However, the hybrid method is not a substitute of an individual calibration of a particular transducer.

Acknowledgments

The investigations presented in this paper were made during a project carried out with the support of the Danish Agency for Technology and Production (FTP).

References

[1] P. M. Juhl, "A numerical investigation of standard condenser microphones", *Journal of Sound and Vibration* **177**, 433-446 (1994).

[2] A. J. Zuckerwar, "Theoretical response of condenser microphones", *Journal of the Acoustical Society of America* **64**, 1278-1285 (1978).

[3] S. Barrera-Figueroa, K. Rasmussen, and F. Jacobsen, "The acoustic center of laboratory standard microphones" *Journal of the Acoustical Society of America* **120**, 2668-2675 (2006).

[4] S. Barrera-Figueroa, K. Rasmussen, and F. Jacobsen, "On experimental determination of the free-field correction of laboratory standard microphones at normal incidence" Metrologia, **44**, 57-63 (2007).

[5] S. Barrera-Figueroa, K. Rasmussen, and F. Jacobsen, "On experimental determination of the random-incidence response of microphones", *Journal of the Acoustical Society of America* **121**, 2628-2636 (2007).

[6] X. Bao, and Y. Kagawa,"A simulation of condenser microphones in free field by boundary element approach", *Journal of Sound and Vibration* **119**, 327-337 (1987).

[7] V. Cutanda-Henríquez, *Numerical Transducer Modeling*, PhD thesis, Ørsted•DTU, Technical University of Denmark, DTU (2002).

[8] R. S. Grinnip III, "Advanced simulation of a condenser microphone capsule", *Journal of the Audio Engineering Society* **54**, 157-66 (2006).

[9] G. Behler and M. Vorlander, "Reciprocal measurements on condenser microphones for quality control and absolute calibration", *Acta Acustica* **90**, 152-160 (2004).

[10] W. R. MacLean, "Absolute measurement of sound without a primary standard", *Journal of the Acoustical Society of America* **12**, 140-146 (1940).

[11] W. Wathen-Dunn, "On the reciprocity free-field calibration of microphones", *Journal of the Acoustical Society of America* **21**, 542-546 (1949).

[12] I. Rudnick and M. N. Stein, "Reciprocity free-field calibration of microphones to 100 kc in air", *Journal of the Acoustical Society of America* **20**, 818-825 (1948).

[13] IEC International Standard 61094-3, Measurement microphone Part 3: Primary method for free-field calibration of laboratory standard microphones by the reciprocity technique (1995).

[14] L. L. Beranek, *Acoustical Measurements* (AIP/ASA) (1988).

[15] H. A. Schenck, "Improved integral formulation for acoustic radiation problems", *Journal of the Acoustical Society of America* **44**, 45-58 (1968).

[16] P. M. Juhl, F. Jacobsen, V. Cutanda, and S. Quiros-Alpera, "On the non-uniqueness problem in a 2-d half-space BEM formulation", *Proceedings of 9th International Congress on Sound and Vibration*, Orlando, Fl., USA (2002).

[17] G. Rasmussen, "The Free Field and Pressure Calibration of Condenser Microphones using Electrostatic Actuator", Brüel & Kjær Technical Review 1969-2, 3-7, (1969).